Visible Light-Driven Photocatalytic Degradation of Rhodamine B over $NaBiO_3$: Pathways and Mechanism

Kai Yu, Shaogui Yang,* Huan He, Cheng Sun,* Chenggang Gu, and Yongming Ju

State Key Laboratory of Pollution Control and Resource Reuse, School of the Environment, Nanjing University, Nanjing 210093, P. R. China

Received: June 2, 2009; Revised Manuscript Received: July 19, 2009

The photocatalytic degradation of rhodamine B (RhB) over $NaBiO_3$ under visible light irradiation was investigated in this study. RhB (20 mg/L) was almost completely decolorized in 30 min in given conditions. It was found that catalyst heating temperature significantly influenced the photocatalytic activity of the catalyst in which crystal water may played an important role, and the original sample exhibited higher activity than the heated samples did. To scrutinize the mechanistic details of the dye photodegradation, several critical analytical methods including UV−vis spectroscopy, HPLC, LC/MS/MS, and GC/MS were utilized to monitor the temporal course of the reaction. All N-deethylation intermediates and several small molecular products were separated and identified. The yield distinctness between two isomer intermediates (DR and EER) was considered to be correlated with the changes in the electron density of the dye molecule. Then two possible competitive photodegradation pathways of RhB over $NaBiO_3$ were proposed: Chromophore cleavage and N-deethylation. Yet, cleavage of dye chromophore structure predominated over the N-deethylation.

Introduction

Because of the great ability to mineralize most of the organic pollutants with low cost,[1] photocatalysis technology as an advanced oxidation process is extensively proposed. Being the most widely studied photocatalyst, TiO_2 possesses several excellent properties such as outstanding oxidative power, photostability, and nontoxicity.[2] Unfortunately, its photoresponse is only limited in the UV region, which accounts for less than 5% of the earth-reaching solar irradiation.[3,4] Consequently, its photocatalytic activity is not high enough for industrial purposes when sunlight is used as the irradiation source. As for the artificial UV light sources, its requirement of large quantities of electrical power would be a high cost in practical application. Therefore, it is very meaningful to develop the visible light response photocatalyst, which can efficiently utilize the inexpensive and inexhaustible solar energy. Following the early study done by Zou et al.,[5] who explored $NiO_x/In_{0.9}Ni_{0.1}TaO_4$ photocatalysis under visible light irradiation, many new vis light-driven photocatalysts were investigated, such as fluorinated Bi_2WO_6 and Ag-loaded $BiVO_4$.[2,6] However, the activities of these novel photocatalysts were not high enough, and the low reaction rate severely hindered the commercialization of this technology.

To avoid the drawbacks, many attempts focused on exploiting and utilizing some new materials with high photocatalytic activity. Perovskite oxides were found to possess high activity under visible light, endowing such materials with extensive application prospect in the treatment of wastewater. Ye and co-workers[7] first reported that $NaBiO_3$ showed a relatively high activity for degradation of methylene blue and 2-propanol due to its strong dispersion in the hybridzed orbitals. Then Kou and co-workers[8] utilized $NaBiO_3$ in photooxidation of polycyclic aromatic hydrocarbons under visible light irradiation in which some optimal experimental condition such as heating temperature was obtained. The proposed compendiary pathways of decomposition of two PAHs seem not to be clear enough to handle the whole photochemical behavior. From the only two articles on $NaBiO_3$-based photocatalysis, the material was thought to be capable of degrading organic pollutant with remarkable performance. To our best insight, however, neither of the articles reported in detail the influence of crystal water on its photocatalytic activity and the mechanisms of the $NaBiO_3$-based photocatalytic degradation of contaminant under visible light.

Triphenylmethane dyes are used extensively in textile, printing, food, and cosmetic industries.[9] The wastewater drained from these industries may cause a dramatic source of aesthetic pollution and may exert long-term adverse effects on the aquatic environment.[10,11] They can persist for a long period in the aquatic environment because of their resistance to chemical and bacterial attacks.[12,13] Rhodamine B (RhB) is a common dye in the triphenylmethane family, which contains four *N*-ethyl groups at either side of the xanthene ring (structure given below). In the present study, it was chosen as the target organic pollutant to investigate its degradation behavior over $NaBiO_3$ under visible light irradiation. The major concern was aimed at the investigation of influence of crystal water on photoactivity of $NaBiO_3$ as well as the separation and identification of the reaction intermediates and the presentation of mechanistic details of the photochemical process. Herein, UV−visible, HPLC, GC/MS, and LC/MS techniques were brought to bear on fulfilling the purpose. In the visible light induced photocatalytic degradation of *N*-ethyl-containing dyes, two different photooxidation pathways, namely N-deethylation and cleavage of the conjugated chromophore structure, were frequently witnessed.[14−16] It was observed that direct cleavage of conjugated chromophore structure predominated in two competitive processes in the present study.

* To whom correspondence should be addressed. Telephone: +86-25-83593239. Fax: +86-25-83593239. E-mail: envidean@nju.edu.cn (C.S.); yangdlut@126.com (S.Y.).

10.1021/jp905173e CCC: $40.75 © 2009 American Chemical Society
Published on Web 08/25/2009

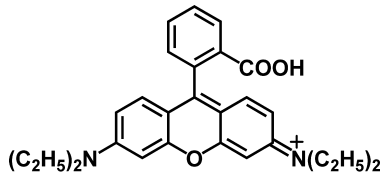

Chemical Structure of RhB

Experimental Section

Materials and Reagents. RhB (laser-grade) was obtained from Acros Chemical Company, and $NaBiO_3 \cdot 2H_2O$ (NBH) was purchased from LI-DE Offset Chemical Material Co. Ltd. All other chemicals were of analytical grade and were used without further purification. Milli-Q water was used throughout this study.

Photoreaction Chamber. Photodegradation experiments were performed in a chamber as shown in Figure 1. A 750-W xenon lamp (Shanghai Hua Lun Lamp Factory) was positioned inside a cylindrical circulating water jacket (quartz) to minimize infrared radiation. The reactor was covered with a 400-nm cutoff (Beijing HZXD Optics Technology Co. Ltd.) and wrapped by the aluminum foil to ensure illumination by visible light only. A 55-W fan was used to keep the chamber at ambient temperature.

Characterization. Crystal structures and optical absorption property were performed using an X-ray diffractometer with Cu Kα radiation (model, Shimadzu LabX XRD-6000) and a UV−vis diffuse reflectance spectrophotometer (Shimadzu UV-2401), respectively. TG-DTA experiment was performed by simultaneous thermal analyzer NETZSCH STA 449 C in N_2 atmosphere at a heating rate of 5 K/min in the temperature range 50−600 °C. Photocatalysts were dispersed in 0.01 M aqueous NaCl solution by sonication for the ζ-potential determining, which was conducted with a ζ-potential analyzer (Zeta PALS, BrookHaven Instruments Corporation).

Photodegradation of RhB. The catalyst samples were prepared by heating commercial NBH at different temperatures for 2 h. An aqueous suspension (100 mL) containing 20 mg/L of RhB and a certain amount of $NaBiO_3$ samples was placed in the reactor. Before irradiation, the suspension was magnetically stirred in the dark for approximately 30 min to ensure the establishment of an adsorption/desorption equilibrium. At given intervals, an appropriate amount of suspension was taken out and filtered through a Millipore filter (pore size 0.22 μm) to remove the solid particles, and the filtrates were collected for analysis.

For comparison, TiO_2 and Bi_2WO_6 were used as reference visible light-driven photocatalysts. TiO_2 was commercial P25, and Bi_2WO_6 was synthesized according to published procedures.[17]

Analytical Methods. The filtrates were analyzed by a Shimadzu UV-2450 spectrophotometer, and the total organic carbon (TOC) was measured by Shimadzu TOC-5000A. The N-deethylated intermediates were detected by HPLC technique (Agilent 1200) equipped with UV−vis diode array detector using a C18 inversed-phase column (150 mm * 4.6 mm i.d., Phenomenex). Ammonium acetate and methanol were used as mobile phase. The gradient elution was programmed as follows: Methanol was obtained at 55% and this proportion was kept for 10 min, then linearly increased to 65% during 0.5 min, then maintained at 65% for 12.5 min and back to 55% in the last 1 min. The flow rate was 1.0 mL/min, and the injection volume was 50 μL. LC-ESI-MS/MS (Thermo) was used to identify the intermediates. The mobile phase was methanol/ammonium acetate solution (75:25, v/v) at a flow rate of 0.2 mL/min. GC/MS analyses were carried out on a Thermo Finnigan Trace gas chromatography interfaced with a Polaris Q ion trap mass spectrometer (Thermo Finnigan). The pretreatment process was as follows: The reaction liquid was filtered and the pH value was adjusted to around 2.5 with HCl. Then the solution was extracted with dichloromethane three times. The extracts were concentrated to 1 mL by rotary evaporation. After the solvent was blown away by the gentle nitrogen, trimethylsilylation was carried out using 0.2 mL of BSTFA-TMCS (99:1) at 50 °C for 30 min.

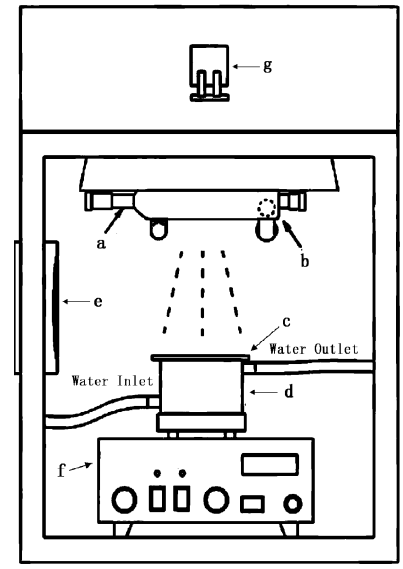

Figure 1. Schematic drawing of the photoreaction system. Xenon lamp (a), circulating water jacket (quartz) (b), UV cutoff (c), reactor (d), cooling fan (e), magnetic stirrer (f), and ballast and power switch (g).

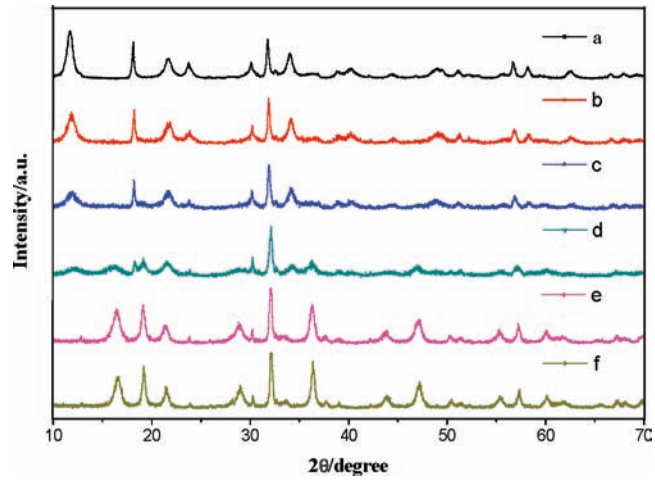

Figure 2. XRD patterns of the samples heated at different temperatures for 2 h. (a) Original sample. Samples heated at (b) 100, (c) 125, (d) 150, (e) 175, and (f) 200 °C.

Results and Discussion

Characterization. XRD was used to examine the crystal structures of the original NBH sample and samples heated at 100, 125, 150, 175, and 200 °C. It can be seen from Figure 2 that pattern (a) was similar to patterns (b) and (c), suggesting that these three samples possess similar crystal structures. The peaks at $2\theta = 11.78°$, $2\theta = 18.2°$, and $2\theta = 32.6°$ of the

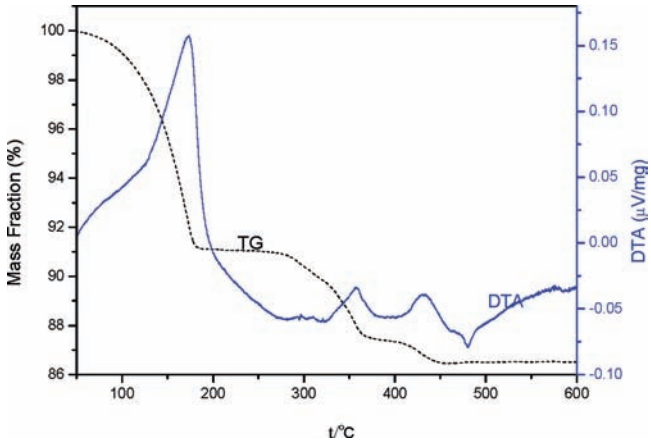

Figure 3. Thermal behavior (dash line for TG curve and solid line for DTA curve) of NBH in nitrogen atmosphere (temperature profile: heating at 5 °C/min to 600 °C).

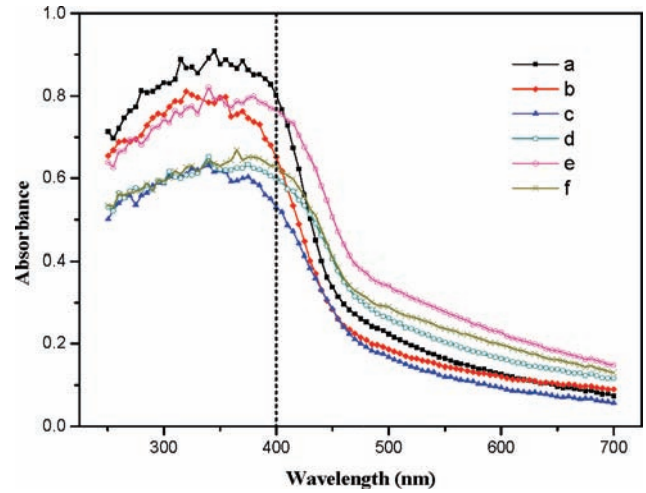

Figure 4. UV−vis diffuse reflectance spectrum of the samples heated at different temperature for 2 h. (a) Original sample. Samples heated at (b) 100, (c) 125, (d) 150, (e) 175, and (f) 200 °C.

samples were in high agreement with those characteristic peaks of standard XRD JCPDS card for $NaBiO_3 \cdot 2H_2O$,[18] and hence crystal water is regarded to be contained in these three samples. It is relevant to note that by increasing the heating temperature to 125 °C, some of the characteristic peak intensities became weak correspondingly. These results indicated that dehydration occurred to a certain degree in the heating process and the 100 and 125 °C heated ones might contain less crystal water than the commercial NBH sample. As a critical state, those characteristic peaks cannot be clearly observed in the pattern of the 150 °C heated sample, while some new diffraction peaks emerged and were considered to be the characteristics of $NaBiO_3$ as expected. The samples heated at 175 and 200 °C had nearly the same patterns, both of which were confirmed to be the fully dehydrated phase, $NaBiO_3$.[7,8]

The TG curve (Figure 3) shows a three-step decomposition process of NBH that is similar to the results reported by Pan et al.[18] The slight difference may be attributed to the different heating rates and particle size used in the present experiment. The first step ending at 183 °C indicates the release of surface water and crystal water. The sharp mass lost in this stage corresponds to the water calculated to be contained in $NaBiO_3 \cdot 2H_2O$. The fact also confirmed the presence of a broad DTA endothermic peak in the same temperature region, which is in accordance with the following formulation:

$$NaBiO_3 \cdot 2H_2O \rightarrow NaBiO_3 \cdot (2 - n)H_2O + nH_2O$$

Clearly, there is not a linear relationship between weight reduction and heating temperature in this stage. The continuous heating process resulted in the acceleration of sample dehydration, which reveals the same information inferred by XRD results. At the region from 183 to 200 °C, the mass reducing rate significantly degreased. Only about 0.06% of the total mass was lost in this period, mainly due to the removal of the residual crystalline water. Thus, the major phase in this stage is still regarded as $NaBiO_3$, which is also consistent with the XRD analysis. The 4.87% reduction in mass recorded between 250 and 600 °C most probably originated from the sample thermal decomposition, which can be illustrated by:[18]

$$NaBiO_3 \rightarrow NaBiO_2 + 0.5O_2$$

A conclusion can be definitely drawn that increasing the temperature to 200 °C resulted in a gradual decrease of sample crystal water content and NBH would lose its crystal water completely in the experimental heating process.

The UV−vis diffuse reflectance spectra of these samples were gained to better understand their photophysical property, and the results are illustrated in Figure 4. The color of the oxide was yellowish, as predicted from the photoabsorption spectrum. Evidently, all six samples had relatively strong absorption around 400 nm, which was followed by a sharp decrease due to the band gap, and the long tail up to about 700 nm was probably caused by the lattice defects.[7] The absorption edge wavelength of NBH was 474 nm, from which the optical band gap energy was estimated by the following equation:[19]

$$E_g = hc/\lambda_0$$

where E_g, h, c, and λ_0 are the band gap energy, Planck's constant, light velocity (m/s), and absorption edge wavelength (nm), respectively. The band gap of NBH was determined to be about 2.62 eV. The other five samples were examined in the same way, and with the heating temperature increased from 100 to 200 °C their band gaps were calculated to be 2.58, 2.45, 2.38, 2.37, and 2.42 eV, respectively.

Activity Comparison. It is all well known that heating has significant influence on the photocatalytic activity of catalyst. Bleaching RhB solution under the same conditions was carried out to determine the different activities of six samples, and the results are shown in Figure 5. It is noticeable that the original sample exhibited a greater activity than the heated samples and with the increase of the sample heating temperature, the RhB degradation rate decreased. For example, the target dye was only decomposed less than 40% with the sample heated at 200 °C in 30 min, while it could be degraded more than 95% with the original one in the same period. Assuming that the photodegradation process followed the pseudo-first-order reaction, the reaction rate constants of RhB over different $NaBiO_3$ samples heated from 100 to 200 °C were calculated to be 0.1042, 0.0747, 0.0462, 0.0257, and 0.0172 min^{-1}, successively. In fact, the highest rate constant belongs to the original one, which was determined to be 0.124 min^{-1}.

On the basis of the above discussion, the crystal water contained in the $NaBiO_3$ samples seems to play an important

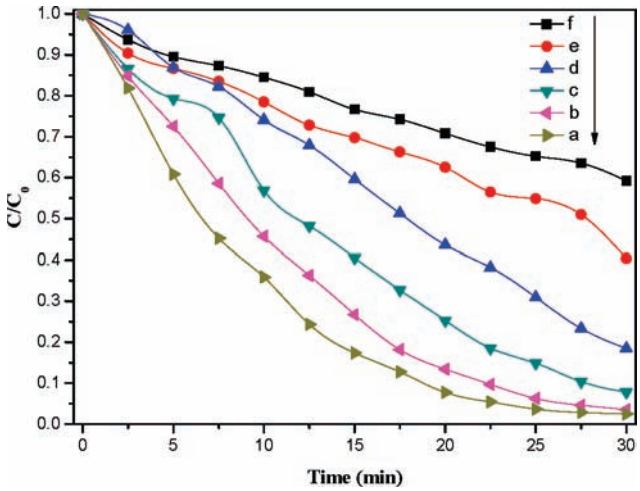

Figure 5. Temporal course of the photodegradation of RhB in aqueous dispersions under visible light irradiation over different samples. (a) Original sample. Samples heated at (b) 100, (c) 125, (d) 150, (e) 175, and (f) 200 °C.

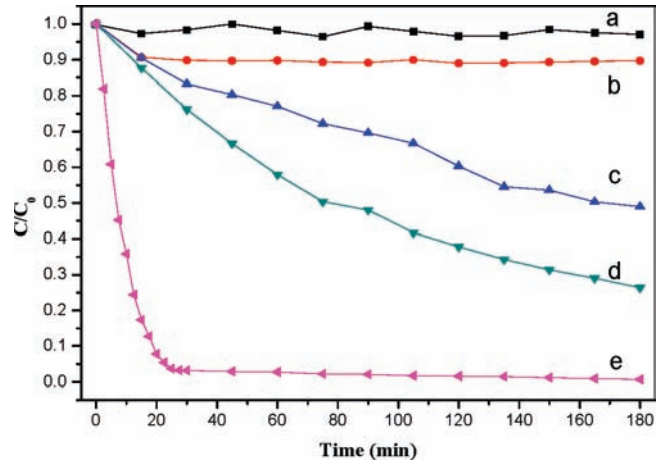

Figure 6. Temporal course of the degradation of RhB under different conditions. Visible light only (a), commercial NBH in darkness (b), TiO_2 under vis irradiation (c), Bi_2WO_6 under vis irradiation (d), and commercial NBH under vis irradiation (e). RhB concentration: 20 mg/L. Catalysts: 1 g/L.

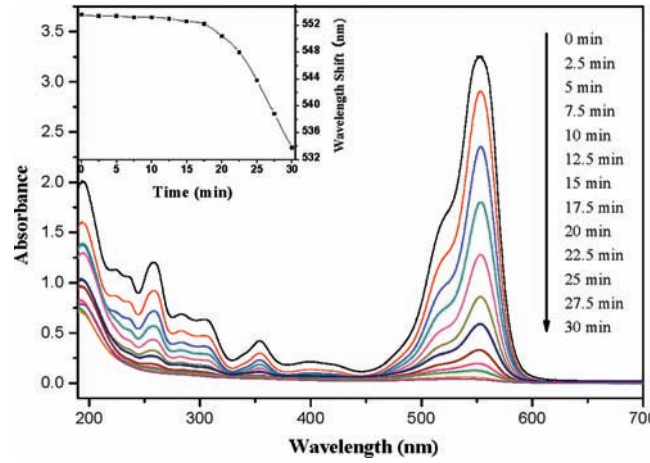

Figure 7. UV−visible spectral changes of RhB in aqueous NBH dispersion as a function of reaction time. Inset: Wavelength shifts as a function of the decrease in absorption maximum.

role in the variation of photoabsorbance property, which actually may affect the photocatalytic activity of the catalyst. Generally, the rate of the photocatalytic reaction is proportional to $(I_\alpha\Phi)^n$ ($n = 1$ for low light intensity and $n = {}^1/_2$ for high light intensity), where I_α is the photon number absorbed by photocatalyst per second and Φ is the efficiency of band gap transition.[20,21] Hence, it can be inferred that increasing I_α resulted in enhanced reaction rate. On the basis of the UV−vis diffuse reflectance spectrum plotted in Figure 4, it can be observed that 100 and 125 °C heated samples showed lower absorbance than NBH did. Their relatively weak photocatalytic activity can be partly explained in terms of a decrease in I_α resulting from poor absorbance in the visible light regions. However, the relatively strong optical absorption above 400 nm appeared at 150, 175, and 200 °C heated samples while they did not exhibit the top activity in the RhB degradation experiment. Taking into account three of them possessing the much smaller forbidden band energy, it can be deduced that the oxidative ability of the photogenerated holes and the reductive ability of the photogenerated electrons must be the worst in all six samples once they were excited by visible light. Thus, from this perspective, it could probably explain the poor activity of these three samples shown in the bleaching experiment.

Control Experiments. The decreases of RhB concentration as a function of reaction time are shown in Figure 6. Control experiments demonstrated that RhB was not degraded in NBH suspension in the dark. Being a typical heterogeneous reaction, the decay of RhB concentration was only witnessed immediately before the reaction and was barely observed after the adsorption−desorption equilibrium of the target was reached. It is well known that the excited state of dye induced by visible light could transfer an electron to an oxygen molecule to generate a superoxide radical anion that can derive many other active oxygen species.[22,23] These active species could lead the degradation of dye to some extent, but it is a very slow and inefficient process that could be ignored in our condition. Figure 7 clearly shows that RhB is relatively stable in aqueous solution under visible light irradiation as expected. Nevertheless, it underwent pronounced decomposition in the presence of NBH under visible light irradiation, from which can be inferred that both visible light and NBH semiconductor particles are indispensable to the photooxidative conversion of RhB.

As a comparison, the results of RhB decoloration over P25 and Bi_2WO_6 under the same irradiation condition are also given in Figure 6. It is obvious that the degradation rates of RhB with TiO_2 and Bi_2WO_6 were much lower. Only 51% RhB can be photodegraded by P25 under visible light in 3 h. Considering that P25 could not directly respond to the irradiation used in the experiment because of its band gap limitation, RhB degraded mostly because of photosensitization between P25 and the dye molecule, which was widely regarded as a low efficiency process. The proportion of degraded RhB can be a little larger when it comes to Bi_2WO_6, which is 74%. The relatively poor photoreaction efficiency might be ascribed to the quick recombination of charge carriers.[6] However, NBH exhibited a much higher photocatalytic activity than the others did. Ninety-seven percent of RhB was photodegraded with the remarkable rate under the same condition in only 30 min and completely bleached in 3 h. The excellent performance could be attributed to the high dispersion in the conduction band composed of the hybridized Na 3s and O 2p orbitals, indicating that the photoinduced electrons have strong mobility on the sp bands.[7,24] This may lead to suppression of the recombination of electron/hole pair and enhancement of the quantum efficiency of photocatalysis.

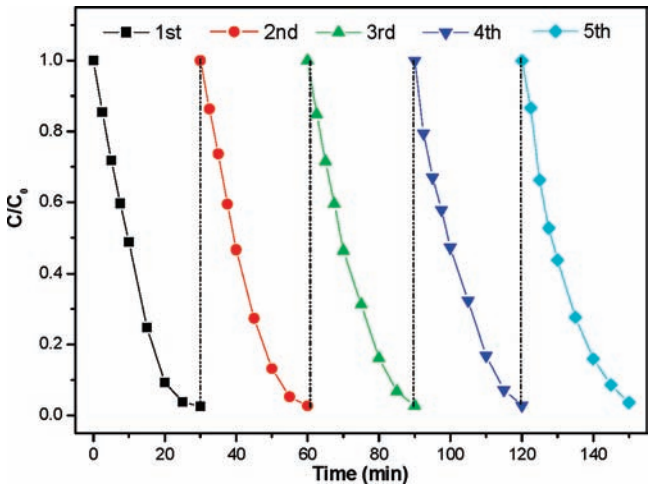

Figure 8. Concentration decrease of RhB during the cycle photodegradation process. RhB concentration: 20 mg/L. Catalysts: 1 g/L.

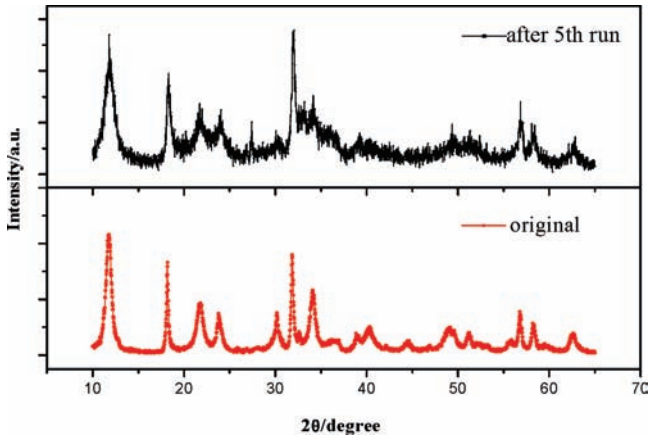

Figure 9. XRD patterns of the NBH before and after RhB bleaching.

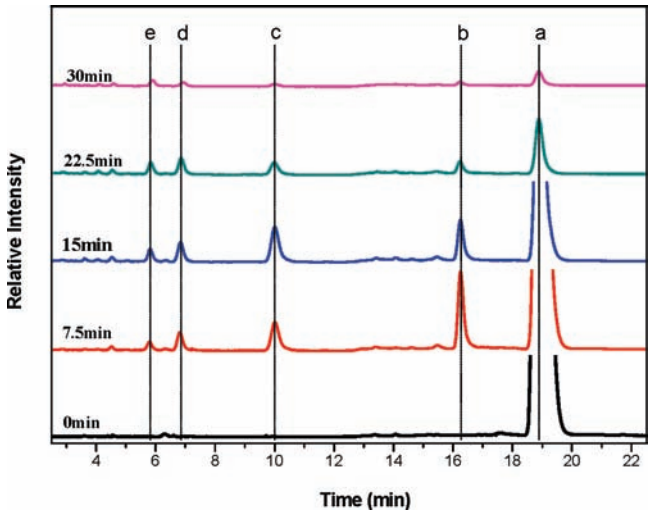

Figure 10. HPLC chromatograms of the N-deethylated intermediates recorded at 520 nm at 0, 7.5, 15, 22.5, and 30 min. Note: *y*-axis is partly enlarged because of the small amount of the N-deethylated intermediates.

In this experiment, NBH exhibited a strong ability to remove RhB. The reaction rate constant of bleaching RhB, 0.124 min^{-1}, is much higher than other studies reported.[25,26] In addition, the TOC removal of RhB reached 21% in 30 min, when dye (20 mg/L) was photooxidated over photocatalysts (1 g/L) under visible irradiation.

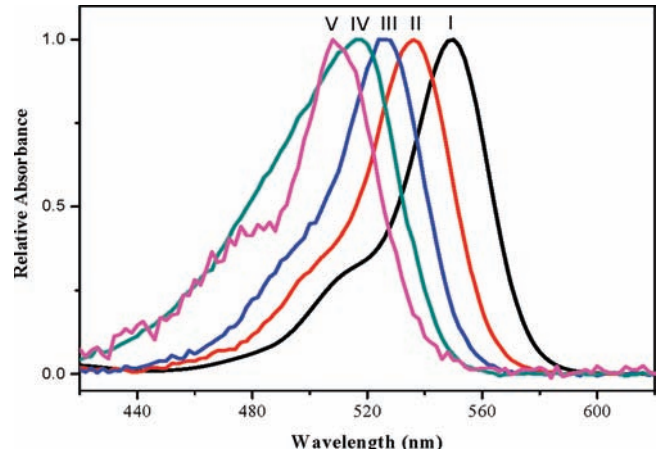

Figure 11. Absorption spectra of N-deethylated intermediates recorded by diode array detector. Spectra I−V correspond to peaks a−e in Figure 10, respectively.

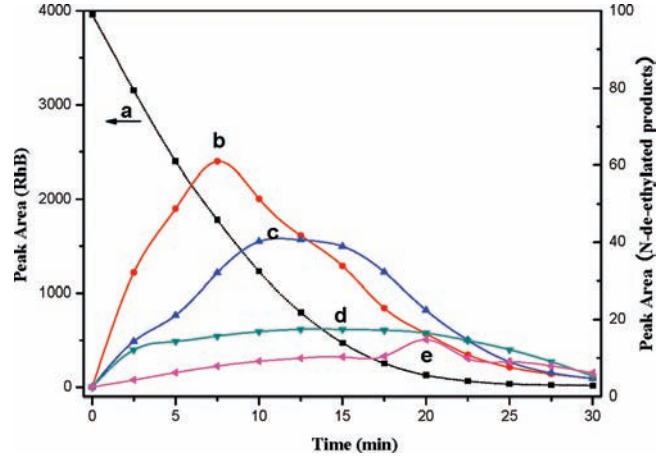

Figure 12. Temporal change in the distribution of the N-deethylated intermediates during the photodegradation. (a) RhB, (b) DER, (b) DR, (d) ER, and (e) R.

UV−Visible Spectra. The UV−visible spectral changes during the photocatalytic degradation of RhB under visible irradiation are listed in Figure 7. As can be seen, the characteristic absorption band of RhB at 554 nm diminished quickly, accompanied by concomitant tiny hypsochromic shifts from 554 to 534 nm of the maximum absorption. Previous studies also reported a similar phenomenon.[27,28] These shifts resulted from the formation of a series of N-deethylated intermediates of RhB, which will be identified and shown in the following results. The sharp decrease in the maximum absorption implies that RhB suffered a rather facile cleavage of the whole conjugated chromophore. The inset shows the wavelength shifts as a function of the absorption maximum. In the early stage during irradiation, because of the high concentration of RhB and the poor yield of N-deethylated intermediates, the absorption band shift can be ignored. However, with further degrading of RhB and the stepwise appearance of the intermediates at the later stage, the blue shift of spectral was more pronounced. The following results support this argument.

Stability Evaluation. Estimating the stability and reusability of catalyst is indispensable for the evaluation of its practical applications. To investigate thedurability of NBH in the reaction, the bleaching experiment was repeated five times. As displayed in Figure 8, RhB was quickly decomposed in each circulation, which suggests that there is no significant loss of activity after five recycles, confirming that NBH is not photocorroded during

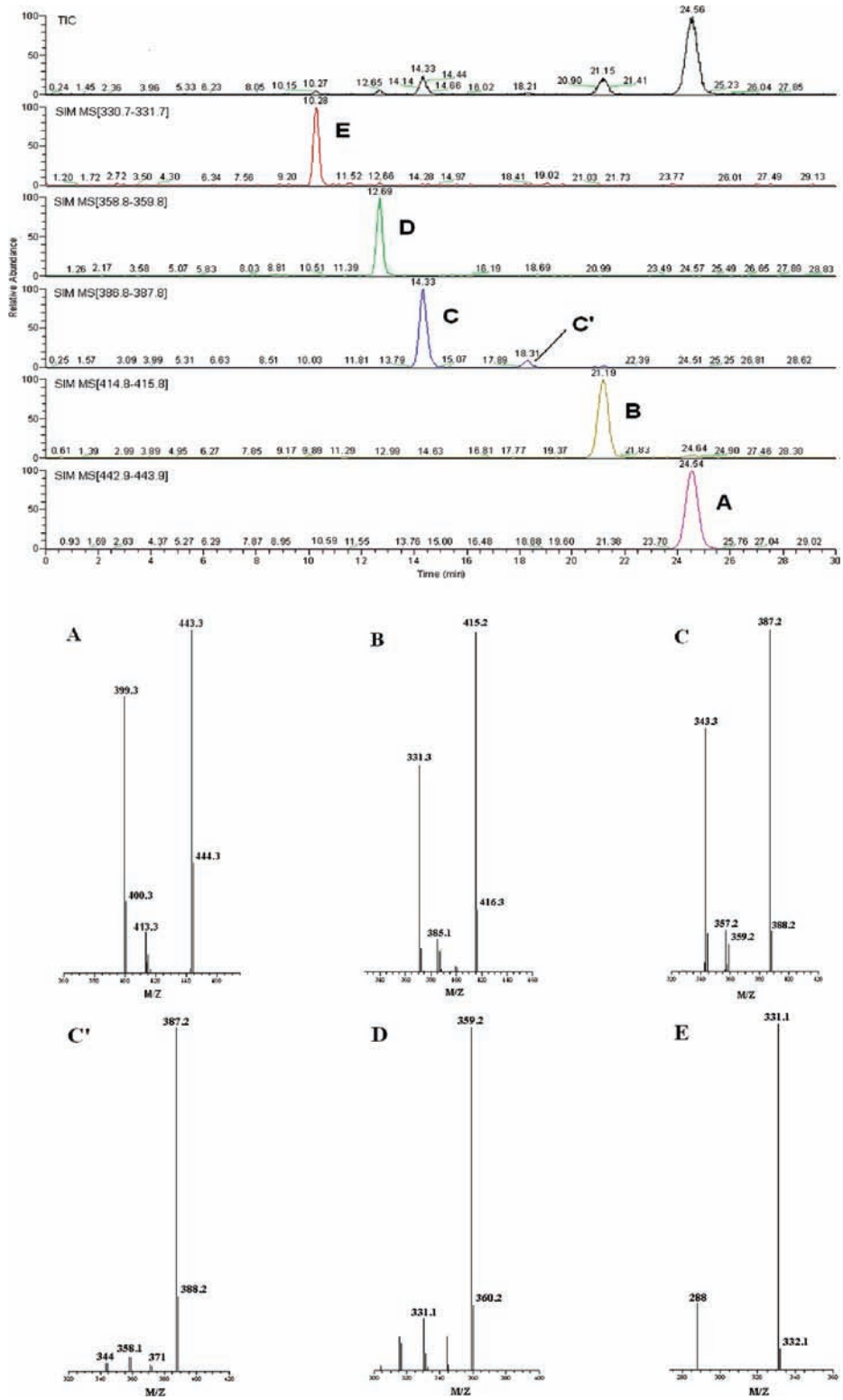

Figure 13. Ion chromatogram (SIM) and MS/MS spectra of N-deethylated intermediates that appeared in the photochemical process. (A) RhB, (B) DER, (C) DR, (C′) EER, (D) ER, (E) R.

the photocatalytic oxidation process. In addition, the XRD analysis of the sample was also surveyed (Figure 9). Little apparent change was observed between the original and the repeated sample pattern, indicating that the crystal structure of the photocatalyst remained unchangeable after the reaction. Judging from these results, NBH was regarded to be stable under the experimental condition.

Separation and Identification of Intermediates. Analyses of the intermediates and final products would help to better comprehend the details of the reaction process. Because of the spectral overlap between the original dye and its degradation intermediates, temporal variations during the photooxidation of RhB were monitored by HPLC equipped with a UV−visible diode array detector at 520 nm. The typical HPLC chromatogram was recorded and shown in Figure 10. In addition to RhB, four N-deethylated intermediates were evidently observed, namely, *N*,*N*-diethyl-*N*′-ethylrhodamine (DER), *N*,*N*-diethylrhodamine (DR), *N*-ethylrhodamine (ER), and rhodamine (R),

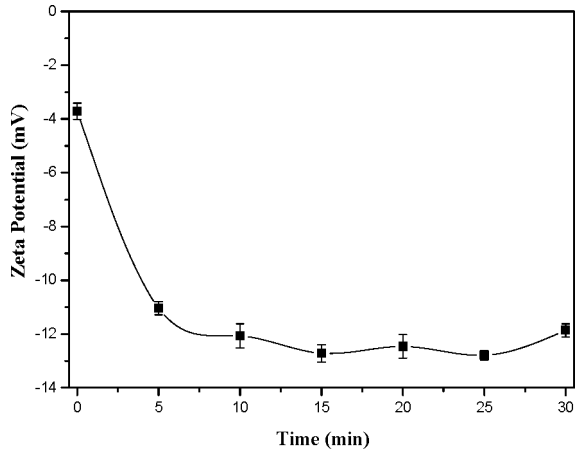

Figure 14. ζ-Potential of the catalyst taken at different times during the reaction.

SCHEME 1: Proposed Specific Adsorption Mode of RhB and DER on the Surface of the Catalyst in Aqueous Dispersion

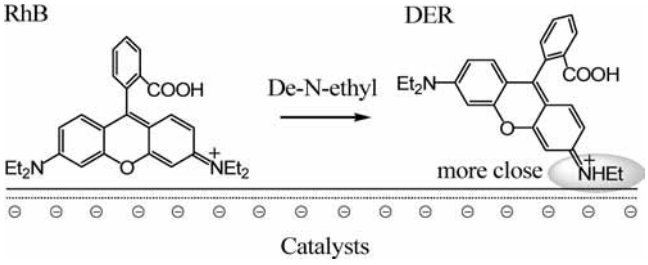

TABLE 1: Identification of the Small Molecular Intermediates of RhB during the Photoreaction by GC/MS

product	R_t (min)	M_w	formula	name
1	5.99	62	$C_2H_6O_2$	ethane-1,2-diol
2	7.54	90	$C_3H_6O_3$	2-hydroxypropanoic acid
3	8.37	90	$C_4H_{10}O_2$	butane-1,3-diol
4	9.17	116	$C_5H_8O_3$	4-oxopentanoic acid
5	13.2	92	$C_3H_8O_3$	propane-1,2,3-triol
6	12.35	122	$C_8H_{10}O$	2,6-dimethylphenol
7	13.65	122	$C_7H_6O_2$	benzoic acid
8	14.2	110	$C_6H_6O_2$	pyrocatechol
9	16.85	132	$C_5H_8O_4$	glutaric acid
10	19.44	146	$C_6H_{10}O_4$	adipic acid
11	21.57	147	$C_8H_5NO_2$	isoindoline-1,3-dione
12	24.42	180	$C_9H_8O_4$	4-(methoxycarbonyl)benzoic acid
13	24.8	180	$C_9H_8O_4$	2-(methoxycarbonyl)benzoic acid
14	25.37	166	$C_8H_6O_4$	phthalic acid
15	25.74	166	$C_8H_6O_4$	isophthalic acid
16	25.96	166	$C_8H_6O_4$	terephthalic acid
17	29.54	170	$C_7H_6O_5$	2,4,6-trihydroxybenzoic acid
18	29.93	278	$C_{16}H_{22}O_4$	dibutyl phthalate

and correspond to peaks a−e, respectively. With the quick disappearance of RhB, the concentration of other intermediates first increased and subsequently decreased with further irradiation, which revealed the formation and the transformation of the reaction intermediates. The characteristic absorption spectra (I−V) of each species are given in Figure 11, corresponding to peaks a−e in Figure 10. The change observed in absorption maximum of the spectral band from 550 nm (spectrum I) to 508 nm (spectrum V) was consistent with the hypsochromic shifts in Figure 7. Considering the auxochromic property of the *N*-ethyl group,[22] the characteristic absorption of the intermediate with less *N*-ethyl was expected to occur at shorter wavelength. A slight deviation between the absorption spectrum recorded in our experiment and those in other reports[15,28] is probably due to the different mobile phases used in elution. The graphical representations of the relative distributions of the N-deethylated intermediates as a function are depicted in Figure 12. The lack of appropriate reference standards and the unavailability of molar extinction coefficients of these intermediates make the precise quantifying of all products hard work. However, we can observe the temporal changes of each N-deethylated intermediate clearly through examining their peak areas in the HPLC chromatograms. Since the start of the illumination reaction, the concentration of the first N-deethylated product (DER) increased and reached the top at 7.5 min and the maximum of DR, ER, and R appeared at 10, 15, and 20 min successively. The variations unambiguously revealed that the N-deethylation of RhB is a stepwise course. Considering that the peak area of RhB was much larger than that of the intermediates in the early stage, as mentioned above, the amount of the N-deethylated products was too small to markedly shift the UV−visible spectral of the whole RhB solution. We can conclude that the N-deethylation process of RhB under visible irradiation over NBH did exist, but it occurred only to a slight extent as observed. Actually the cleavage of the whole conjugated chromophore structure of RhB dominated the photoreaction.

The N-deethylated intermediates were further confirmed using the LC-ESI-MS/MS method. Displayed in Figure 13, all the products identified by HPLC were clearly recorded in the ion chromatogram and corresponding MS/MS spectra are also given. The mass peaks at *m*/*z* 443, 415, 387, 359, and 331 are those of RhB and its N-deethylated intermediates. These peaks differ exactly by 28 mass units successively, which consist of the sequential N-deethylation of maternal RhB. It is relevant to note that when the solution was monitored at the $m/z = 387$ mode, two peaks (C and C′) appeared in the ion chromatogram. Both of them were regarded to be the intermediates that possess two less ethyl groups relative to the RhB dye. One of the isomers lost two ethyl groups at the same side of RhB, noted as DR; the other one formed by removal of an ethyl group from each side of the RhB molecule, N-ethyl-N'-ethylrhodamine, noted as EER (detection limit of DAD is not low enough to examine such small quantity species). EER species is expected to be eluted off the LC column after DR because of its weaker polarity.[29]

It is noteworthy that the peak area of EER is smaller than that of DR in the ion chromatogram (Figure 13), which means DR predominated over EER to be the major dediethyl product of RhB during the reaction process. A similar result was found in earlier studies.[12,15] Three possible causes of this phenomenon were first proposed. (1) As well known, the p-type electron orbit of nitrogen would conjugate to the p-type electron orbit of the benzene ring to form a conjugative system. On account of the electron-donating property of ethyl and the hyperconjugation effect, the ethyl groups might be affected by the conjugative system. When the first ethyl was removed, the electronic delocalization over the one ethyl side was weakening. Therefore, this side of the DER molecule seems relatively unstable. (2) As mentioned above, the removal of an ethyl would transform the electron atmosphere and the higher electron density was supposed to appear at the two ethyl sides, thus the one ethyl side was regarded to be the positive center. This side is easier to be adsorbed on the surface of the catalyst through electrostatic interaction.[14,15] To support this viewpoint, the ζ-potential of the photocatalysts during the reaction was measured by ζ-potential analyzer. The results plotted in Figure 14 reveal that the surface of the catalyst was negatively charged under the experimental

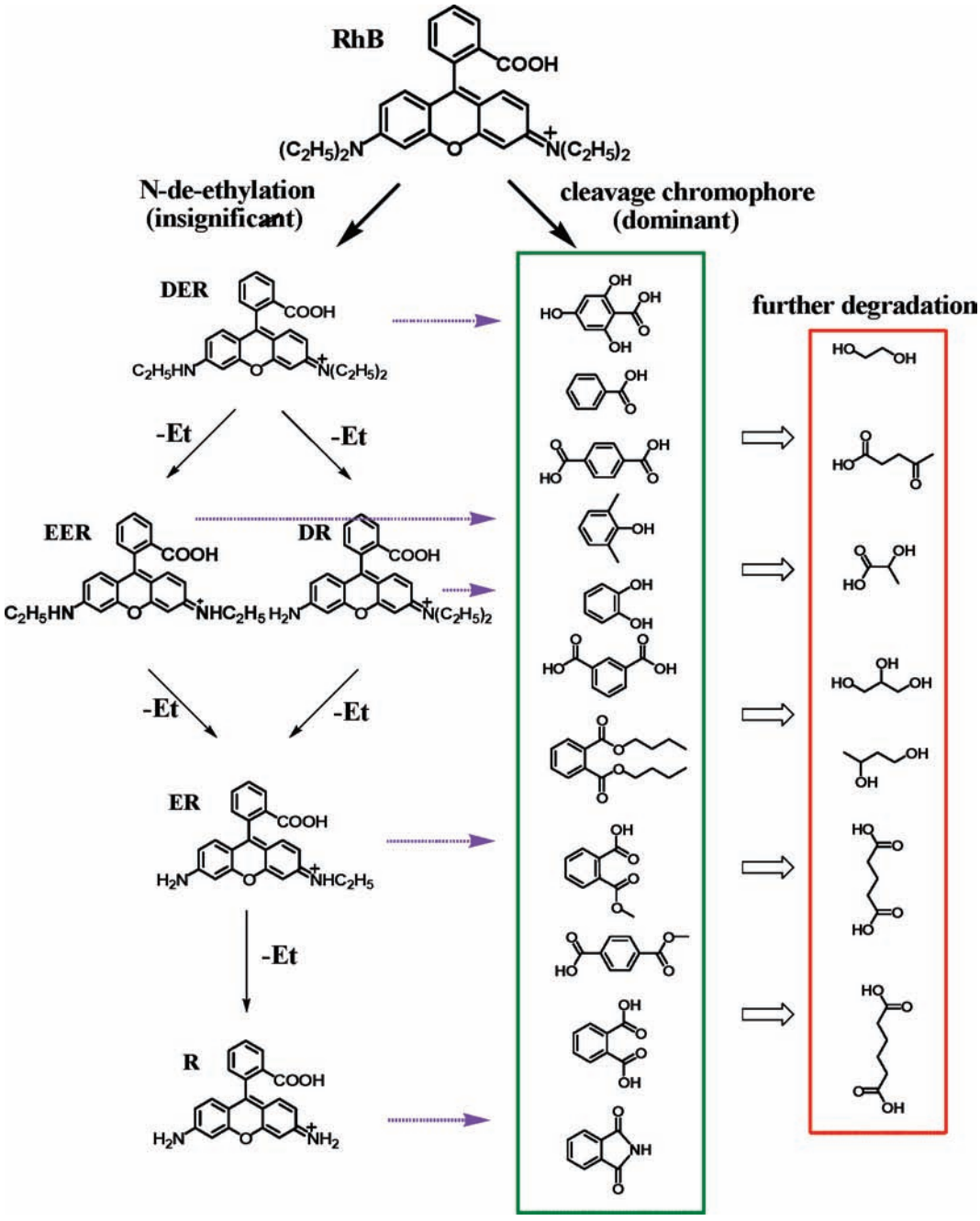

Figure 15. Proposed pathway of RhB in NBH suspension irradiated by visible light.

condition. Therefore, positively charged ethylamine group was preferential to be adsorbed on the surface of the catalyst (shown in Scheme 1), and the active species have strong advantages to attack the nearer groups. (3) The two ethyls connected on the same nitrogen atom might sterically hinder active radical attack on the nitrogen atom in the diethylamine group. Thereby, the second detached ethyl was prone to be loosened at the same side where RhB eliminated its first ethyl.

As the conjugated chromophore structure was wrecked, the reaction mixture became more complex, which was attributed to the formation of some highly polar and small molecular intermediates. GC/MS technique was used for further analyses to obtain more information about these products. After all the peaks in the chromatograms were carefully examined, 18 compounds were identified as possible intermediates on the basis of the information given by the commercial library (NIST2). Detailed data are listed in Table 1. They were mainly organic acids and various alcohols, such as benzoic acid and butane-1,3-diol. These products can be abundant proof that RhB not only lost *N*-ethyl but also suffered advanced degradation. The partial intermediates determined here were also identified in previous studies.[12,30]

Photodegradation Pathway of RhB. Under visible light irradiation, two competitive processes occurred simultaneously during the photoreaction: N-deethylation and destruction of dye chromophore structure.[31] According to earlier reports,[32,33] most N-deethylation processes are preceded by formation of a nitrogen-centered radical while destruction of dye chromophore structures is preceded by generation of a carbon-centered radical. The question as to which kind of radical is mainly formed (nitrogen-centered radical or carbon-centered radical) is determined by the hydrolysis or deprotonation suffered by dye cation radicals, which in turn are defined by the different adsorption modes of RhB on the catalyst surface.

On the basis of all the above experimental results and the previous studies,[16,22,29,34] we tentatively propose the pathway for the visible light induced photocatalytic degradation of RhB as depicted in Figure 15. It clearly appears that the dye molecule in the reaction suspension would adsorb on the particle surface through the positively charged diethylamine function. The first step probably involved N-deethylation process. Five *N*-deethyl products were identified during the photooxidative reaction, and the successive appearance of the maximum of each intermediate (Figure 13) reveals that the N-deethylation of RhB is a stepwise process.

On the other hand, Figure 12 also offers the information that the rather facile chromophore cleavage of the dye molecule simultaneously occurred through the whole degradation process. This might be ascribed to the excellent photocatalytic activity that NBH possessed. The photogenerated active species such as $^{\bullet}OH$ or photogenerated hole could directly attack the central carbon of RhB to decolorize the dye rapidly to some degree. Furthermore, it is entirely possible for these active species to work on any N-deethylation intermediates likewise while the deethylation process was continuing. Some primary oxidation products such as adipic acid, phthalic acid, isophthalic acid, and terephthalic acid were originated from this period. These compounds were further degraded into smaller compounds during the decolorization process, including ethane-1,2-diol, butane-1,3-diol, propane-1,2,3-triol, and so forth. Then the small molecules were mineralized to form CO_2 and H_2O, which can be proved by the results of the TOC measurement.

Overall, results of the present study show that the $NaBiO_3$-based photooxidation treatment of RhB solution under visible light irradiation may involve two competitive processes, namely N-deethylation and chromophore cleavage. Both ways happened simultaneously and could lead the RhB molecule toward colorless compounds and eventually to CO_2 and H_2O. Considering the quick disappearance of RhB and the slight amount of N-deethylation intermediates generated, it is reasonable to postulate that the cleavage way is the predominant reaction route in our experiment.

Conclusions

RhB could be easily decolorized by $NaBiO_3$ under visible light irradiation. In our experiment, $NaBiO_3 \cdot 2H_2O$ exhibited a higher photoactivity than that of heated $NaBiO_3$ samples. The characterization data indicated that the crystal water contained in the catalyst has significant effect on its photocatalytic activity. RhB (20 mg/L) was decomposed about 97% under visible light over $NaBiO_3 \cdot 2H_2O$ (1 g/L) in 30 min, which was much more efficient than Bi_2WO_6 and P25 performed under the same condition. Five N-deethylated intermediates of RhB including two isomers (DR and EER) were monitored by LC-ESI-MS/MS. It was proposed that the different yields of these two isomers were mainly derived from the transformation of the electron atmosphere over the RhB molecule. Moreover, 18 small molecular products were also identified by GC/MS. On the basis of the data collected, the mechanism of RhB photodegradation on $NaBiO_3 \cdot 2H_2O$ has been elucidated that the decomposition occurred via two competitive pathways, yet chromophore cleavage predominated over N-deethylation to be the major reaction route.

Acknowledgment. This research was supported by the National Natural Science Foundation of China (20737001 and 20707009), the China Ministry of Science and Technology (MOST) National Research Initiative Grants Program for State Key Laboratories, and Opening Foundation for Key Laboratory of Industrial Ecology and Environmental Engineering (No. 0703).

References and Notes

(1) Stylidi, M.; Kondarides, D. I.; Verykios, X. E. *Appl. Catal., B* **2004**, *47*, 189.
(2) Kohtani, S.; Tomohiro, M.; Tokumura, K.; Nakagaki, R. *Appl. Catal., B* **2005**, *58*, 265.
(3) Chatterjee, D.; Dasgupta, S. *J. Photochem. Photobiol., C* **2005**, *6*, 186.
(4) Zhao, D.; Chen, C.; Wang, Y.; Ma, W.; Zhao, J.; Rajh, T.; Zang, L. *Environ. Sci. Technol.* **2008**, *42*, 308.
(5) Zou, Z. G.; Ye, J. H.; Sayama, K.; Arakawa, H. *Nature* **2001**, *414*, 625.
(6) Fu, H. B.; Zhang, S. C.; Xu, T. G.; Zhu, Y. F.; Chen, J. M. *Environ. Sci. Technol.* **2008**, *42*, 2085.
(7) Kako, T.; Zou, Z. G.; Katagiri, M.; Ye, J. H. *Chem. Mater.* **2007**, *19*, 198.
(8) Kou, J. H.; Zhang, H. T.; Li, Z. S.; Ouyang, S. X.; Ye, J. H.; Zou, Z. G. *Catal. Lett.* **2008**, *122*, 131.
(9) Vinod, K. N.; Puttaswamy, T.; Gowda, K. N. N. *J. Mol. Catal. A: Chem.* **2009**, *298*, 60.
(10) Ayed, L.; Chaieb, K.; Cheref, A.; Bakhrouf, A. *World J. Microbiol. Biotechnol.* **2009**, *25*, 705.
(11) Waldau, L. *Kem. Tidskr.* **1979**, *91*, 20.
(12) He, Z.; Sun, C.; Yang, S.; Ding, Y.; He, H.; Wang, Z. *J. Hazard. Mater.* **2009**, *162*, 1477.
(13) Li, L.; Dai, W. K.; Yu, P.; Zhao, J.; Qu, Y. B. *J. Chem. Technol. Biotechnol.* **2009**, *84*, 399.
(14) Wang, Q.; Chen, C. C.; Zhao, D.; Ma, W. H.; Zhao, J. C. *Langmuir* **2008**, *24*, 7338.
(15) Chen, F.; Zhao, J. C.; Hidaka, H. *Int. J. Photoenergy* **2003**, *5*, 209.
(16) Hu, X. F.; Mohamood, T.; Ma, W. H.; Chen, C. C.; Zhao, J. C. *J. Phys. Chem. B* **2006**, *110*, 26012.
(17) Liu, S.; Yu, J. *J. Solid State Chem.* **2008**, *181*, 1048.
(18) Pan, J. Q.; Sun, Y. Z.; Wan, P. Y.; Wang, Z. H.; Liu, X. G. *Electrochim. Acta* **2006**, *51*, 3118.
(19) Mills, A.; Davies, R. H.; Worsley, D. *Chem. Soc. Rev.* **1993**, *22*, 417.
(20) Hattori, A.; Tada, H. *J. Sol-Gel Sci. Technol.* **2001**, *22*, 47.
(21) Huang, G. L.; Zhu, Y. F. *J. Phys. Chem. C* **2007**, *111*, 11952.
(22) Chen, C.; Zhao, W.; Li, J.; Zhao, J.; Hidaka, H.; Serpone, N. *Environ. Sci. Technol.* **2002**, *36*, 3604.
(23) Fu, H. B.; Pan, C. S.; Yao, W. Q.; Zhu, Y. F. *J. Phys. Chem. B* **2005**, *109*, 22432.
(24) Mizoguchi, H.; Woodward, P. M. *Chem. Mater.* **2004**, *16*, 5233.
(25) Yu, J. G.; Yu, X. X. *Environ. Sci. Technol.* **2008**, *42*, 4902.
(26) Zhang, C.; Zhu, Y. F. *Chem. Mater.* **2005**, *17*, 3537.
(27) Wu, T. X.; Liu, G. M.; Zhao, J. C.; Hidaka, H.; Serpone, N. *J. Phys. Chem. B* **1998**, *102*, 5845.
(28) Horikoshi, S.; Saitou, A.; Hidaka, H.; Serpone, N. *Environ. Sci. Technol.* **2003**, *37*, 5813.
(29) Chen, C. C.; Zhao, W.; Lei, P. X.; Zhao, J. C.; Serponer, N. *Chem.—Eur. J.* **2004**, *10*, 1956.
(30) Lei, P. X.; Chen, C. C.; Yang, J.; Ma, W. H.; Zhao, J. C.; Zang, L. *Environ. Sci. Technol.* **2005**, *39*, 8466.
(31) Perez-Estrada, L. A.; Aguera, A.; Hernando, M. D.; Malato, S.; Fernnandez-Alba, A. R. *Chemosphere* **2008**, *70*, 2068.
(32) Liu, G. M.; Li, X. Z.; Zhao, J. C.; Hidaka, H.; Serpone, N. *Environ. Sci. Technol.* **2000**, *34*, 3982.
(33) Mai, F. D.; Chen, C. C.; Chen, J. L.; Liu, S. C. *J. Chromatogr., A* **2008**, *1189*, 355.
(34) Chen, C. C.; Fan, H. J.; Jan, J. L. *J. Phys. Chem. C* **2008**, *112*, 11962.

JP905173E